

## Granular clustering in a hydrodynamic simulation

Scott A. Hill and Gene F. Mazenko

*James Franck Institute and Department of Physics, University of Chicago, Chicago, Illinois 60637, USA*

(Received 25 June 2002; revised manuscript received 20 March 2003; published 11 June 2003)

We examine the hydrodynamics of a granular gas using numerical simulation. We demonstrate the appearance of shearing and clustering instabilities predicted by linear stability analysis, and show that their appearance is directly related to the inelasticity of collisions in the material. We discuss the rate at which these instabilities arise and the manner in which clusters grow and merge.

DOI: 10.1103/PhysRevE.67.061302

PACS number(s): 45.70.Mg

One of the key differences between a granular material and a regular fluid is that the grains of the former lose energy with each collision, whereas the molecules of the latter do not. Even when the inelasticity of the collisions is small, it can give rise to dramatic effects, such as the *Maxwell Demon* effect [1] and, the topic of this paper, the phenomenon of granular clustering. Experiments [2,3] and molecular dynamics simulations [4] alike show that low-density collections of grains (“granular gases”) in the absence of gravity do not become homogeneous with time, but instead form denser clusters of stationary particles surrounded by a lower-density region of more energetic particles. A kinetic explanation for this behavior is that, when a particle enters a region of slightly higher density, it has more collisions, loses more energy, and so is less able to leave that region. This increases the local density and makes it more likely that additional particles are captured in the same way.

We are interested in describing this clustering behavior using hydrodynamics. There is considerable work [5] deriving granular hydrodynamics from kinetic theory, focusing on analytical treatments of the long-wavelength behavior of the system. Goldhirsch and Zanetti [4], for instance, describe clustering as the result of a hydrodynamic instability: a region of slightly higher density has more collisions, so more energy is lost and the region has a lower “temperature” [6]. Less temperature results in less pressure, and this lower-pressure region, in turn, attracts more mass from the surrounding higher-pressure regions. Their paper uses long-wavelength stability analysis to show that, in a system of hydrodynamic equations similar to Eq. (1) below, higher-density regions do indeed have lower pressure, fuelling the instability.

In this paper, we study the hydrodynamics of granular clustering in zero gravity, by using numerical simulation. Our motivation is to determine whether a coarse-grained description, in terms of local particle, momentum, and energy densities, can be used to treat characteristic behaviors of granular materials as a self-contained dynamical system [7]. We show that the instabilities predicted by linear analysis do arise in our simulations, and discuss how the onset of these instabilities depends on the inelasticity of collisions in the material. We also show the manner in which clusters develop.

We begin with a number density field  $\rho$ , a flow velocity field  $\mathbf{u}$ , and a temperature [6] field  $T$ . These are related by a standard set of hydrodynamic equations for granular materials, introduced by Haff [8]:

$$\begin{aligned} \frac{\partial \rho}{\partial t} &= -\nabla_i(\rho u_i), \\ \frac{\partial(\rho u_i)}{\partial t} &= -\nabla_i P - \nabla_j(\rho u_i u_j) + \nabla_j(\eta_{ijkl} \nabla_k u_l), \\ \frac{\partial T}{\partial t} &= -\nabla_i(u_i T) + \frac{1}{\rho} \nabla_i(\tilde{\kappa} \nabla_i T) + \frac{1}{\rho} \eta_{ijkl}(\nabla_i u_j)(\nabla_k u_l) - \tilde{\gamma} T, \end{aligned} \quad (1)$$

where repeated indices are summed over and where  $P$  is pressure,  $\tilde{\kappa}$  is the bare thermal conductivity, and  $\eta_{ijkl} = \tilde{\eta}(\delta_{ik}\delta_{jl} + \delta_{il}\delta_{kj} + \delta_{ij}\delta_{kl})$  is the isotropic bare viscosity tensor. These equations bear much in common with those for normal fluids [9]. The most important addition is that of the term  $-\tilde{\gamma}T$ , which accounts for the inelasticity of collisions; parameter  $\tilde{\gamma}$  is proportional to  $(1-r^2)$ , where  $r$  is the coefficient of restitution. Using kinetic theory results [8], the transport coefficients are chosen to depend on temperature and density:

$$\begin{aligned} \tilde{\kappa} &= \kappa T^{1/2}, \\ \tilde{\eta} &= \eta \rho T^{1/2}, \\ \tilde{\gamma} &= \gamma T^{1/2}. \end{aligned} \quad (2)$$

Typically, work in granular hydrodynamics is done in low-density regimes, where grains may be treated as point particles interacting via collisions. When simulating aggregation, however, one must take excluded volume into account. We do this by introducing a barrier in pressure  $P(\rho)$  at some maximum (close-packed) density  $\rho_0$ . This is in addition to the usual hydrodynamic pressure  $\rho T$ . We choose, in particular, the simple quadratic form

$$P = \rho T + U(\rho^2 - \rho_0^2)\theta(\rho - \rho_0), \quad (3)$$

where  $U$  is a positive parameter,  $\theta(x)$  is the unit step function, and  $\rho_0$  is the close-packed density. This method, which we introduced in an earlier paper [10], is a simple way to model the incompressibility of the system at high densities [11].

We evaluate our equations in two dimensions using a finite-difference Runge-Kutta method, on a square lattice

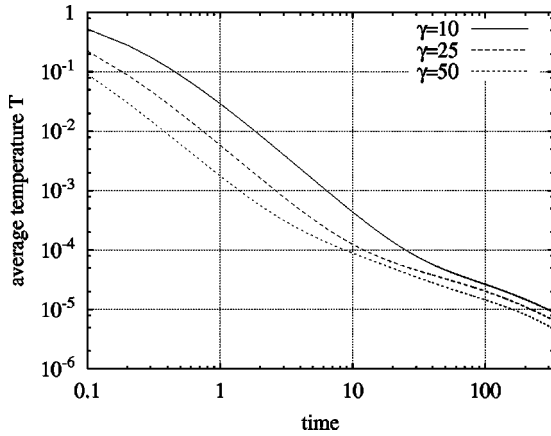


FIG. 1. The evolution of the average temperature of the system over time for three different values of the inelasticity parameter  $\gamma$ , on a log-log plot. Note that in our simulations all variables are considered dimensionless.

with periodic boundary conditions. (See Ref. [12] for more details.) The lattice spacing is chosen to be large enough so that each site contains a number of grains, and we can consider the density to be a continuous variable. We start with random initial conditions  $\rho = 0.1 + 0.001r_1(z, x)$ ,  $u_z = r_2(z, x)$ ,  $u_x = r_3(z, x)$ , and  $T = 1 + 0.1r_4(z, x)$ , where  $r_i(z, x)$  are random numbers chosen between  $-1$  and  $1$ . The model's other parameters for the data presented here are  $\eta_0 = 25$ ,  $\kappa_0 = 1$ ,  $U = 4 \times 10^4$ ,  $\rho_0 = 0.2$ , and  $\gamma$  taking on several different values. All numbers given here are in dimensionless units [13]. Our time step in these units is  $\Delta t = 10^{-3}$ .

We begin with a system that is  $64 \times 64$  in size. The homogeneous state with which we initialize our system is already a solution to the above equations. In this initial homogeneous cooling state, the velocity and all gradients vanish, and the temperature decays with time due to the inelasticity. Equation (1) reduces to

$$\frac{\partial T}{\partial t} = -\gamma T^{3/2}, \quad (4)$$

which yields *Haff's cooling law*,  $T(t) = T(0)(1 + t/t_0)^{-2}$ . This state is seen universally in simulations [14–17], but only initially, for it is unstable to hydrodynamic modes [4], resulting in a long-range shear flow followed by the clustering instability mentioned above.

Figure 1 shows the decay of the average temperature as a function of time in our simulation for three different values of the inelasticity parameter  $\gamma$ . The initial decay approximately follows the predicted  $-2$  exponent (Fig. 2), while for later times the temperature decays at a slower rate as the instabilities agitate the system [15,16]. In the limit of low inelasticity, the maximal rate of decay more closely approaches Haff's predicted inverse-square behavior (Fig. 2). (Note, however, that the temperature will not decay at all in a completely elastic system.) In more inelastic systems, the hydrodynamic instabilities kick in sooner and compromise the homogeneity of the system. One could characterize the time it takes for the instabilities to emerge by the time it

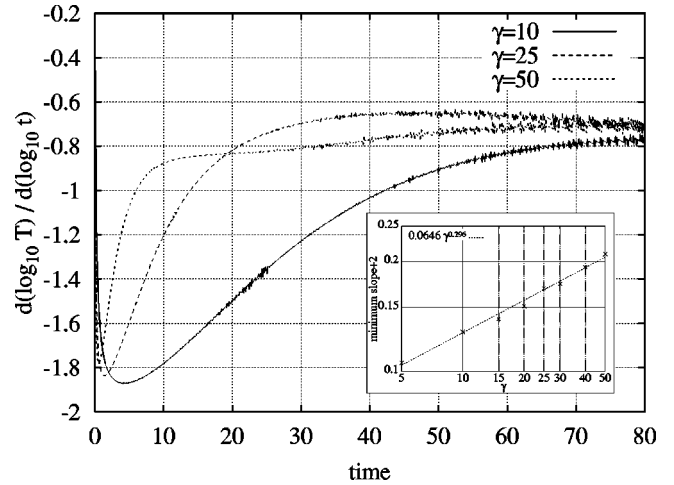


FIG. 2. The logarithmic derivative of  $T(t)$ ; that is,  $d(\log_{10} T)/d(\log_{10} t)$ . This derivative gives the slope of the lines in the first graph, or equivalently, the exponent of the power-law decay rate. Despite appearances, the curves on the right side of the second graph are approaching maxima, not asymptotes. (The  $\gamma = 50$  curve does not converge to a constant value even through  $t = 1000$ , which is as long as our simulations have run.) The inset shows that the maximum power-law decay rate (i.e., the minima of each curve in the main graph) approaches the predicted value of  $-2$  as the system becomes more elastic, as  $\gamma^{0.3}$ .

takes for the temperature to reach its fastest decay rate. Figure 3 shows that this onset time decreases with respect to the inelasticity parameter as a power law with an exponent of  $-4/3$ . One may compare this to the work in Ref. [16], where by matching asymptotic limits they conclude that the onset time of instability depends on the inelasticity parameter as a power law with an exponent of  $-2$ , in the dilute, elastic limit.

The first instability that is predicted to dominate the homogeneous solution is a hydrodynamic shearing mode: two

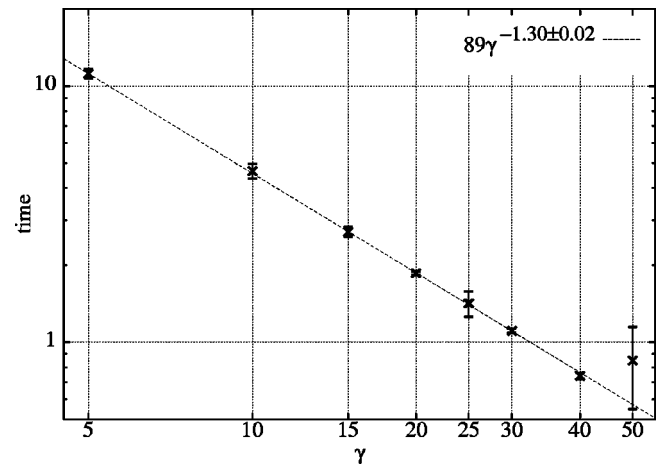


FIG. 3. The time at which the decay rate of the temperature reaches maximum, as a function of  $\gamma$ . The errors are rounding errors due to the finite sample rate. The onset time seems to depend on the inelasticity parameter according to a power law with exponent  $-1.30 \pm 0.02$ .

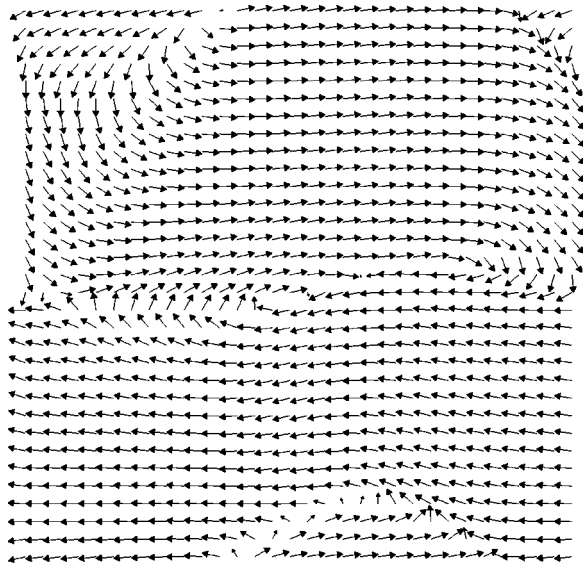


FIG. 4. A flow diagram for  $\gamma=50$  at  $t=450$ . Each arrow represents the average velocity of four lattice sites to improve readability.

bands of material moving in opposite directions. This has been seen in several molecular dynamic simulations [14,17]; Fig. 4 shows how it has developed in our system as two horizontal shear bands. Figure 5 shows that our system develops a clustering instability as well. Note that the single cluster takes on a compact shape, which is surprising given that there is no surface tension in our model. If clusters are supposed to grow by accretion, then one would expect a ramified structure. If we consider a larger system, as in Fig. 6, we find that several compact clusters form in the same manner as that in Fig. 5. As time goes on, however, these clusters reach out to their neighbors, stretching into the more stringlike forms seen in simulation [4]. In hindsight, we are

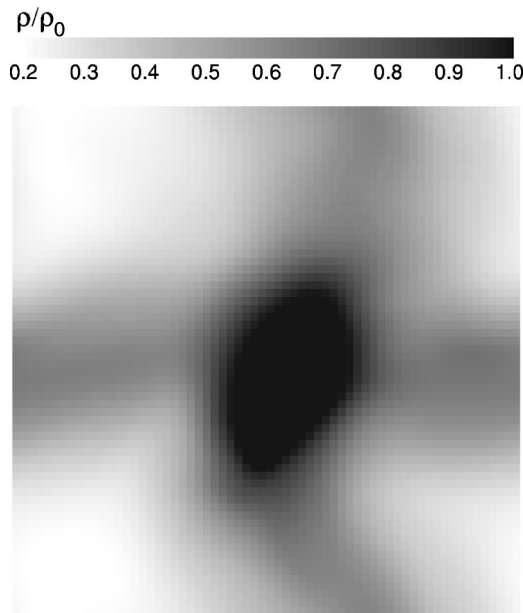


FIG. 5. The density distribution for the  $\gamma=50$  system at time  $t=100$ .

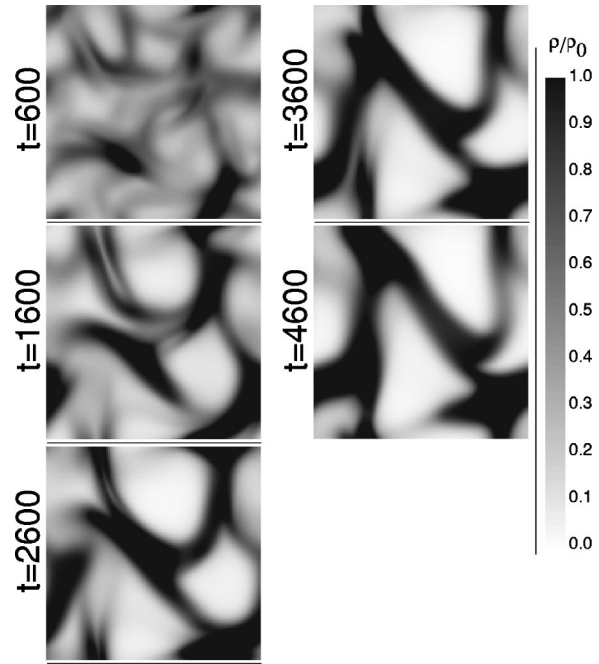


FIG. 6. The density distribution for a large ( $128 \times 128$ ) system at several times during its evolution.

able to see this behavior in the smaller system as well, where the single cluster interacts with itself through the periodic boundaries.

Finally, to demonstrate that this clustering instability is the result of the inelastic parameter, we compare the width of the density distribution for inelastic systems with the distribution for the elastic case  $\gamma=0$  (Fig. 7). In the absence of inelasticity, the density distribution collapses to a delta function, indicating complete homogeneity.

Our results show that the shearing and clustering instabilities, identified by Goldhirsch and Zanetti using a simplified version of the above equations, exist in the complete nonlin-

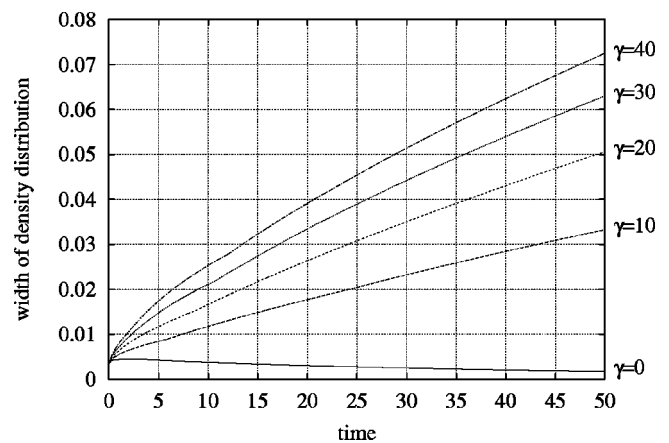


FIG. 7. The width of the density distributions (i.e.,  $\rho_{max} - \rho_{min}$ ) for several values of  $\gamma$ , including the elastic case  $\gamma=0$ . Notice that the density distribution is collapsing to a delta function in the elastic case, approaching complete homogeneity, while the inelastic systems show broadening density distributions due to the clustering instability.

ear granular hydrodynamic equations (1). Haff's cooling law is obeyed in the limit of small inelasticity, but, in general, the instabilities become relevant before the system has a chance to completely homogenize. The power-law dependence of the onset time for these instabilities on the inelasticity, and the  $-4/3$  exponent in particular, are interesting; we have not found any reference to these in the literature. Also interesting is the way in which these clusters develop from compact structures into networks that span the system. It is not clear whether an individual cluster begins to stretch out because of

the proximity of its neighbors, or because of effects due to its increasing surface size. One can imagine that the behavior of this system could change as we alter the total amount of mass in the system.

We thank Professor Todd DuPont for his assistance in constructing our simulations, and Professor Heinrich Jaeger, Professor Sidney Nagel, and Professor Thomas Witten for helpful conversations. This work was supported by the Materials Research Science and Engineering Center through Grant No. NSF DMR 9808595.

- 
- [1] J. Eggers, Phys. Rev. Lett. **83**, 5322 (1999).
- [2] A. Kudrolli, M. Wolpert, and J.P. Gollub, Phys. Rev. Lett. **78**, 1383 (1997).
- [3] J.S. Olafsen and J.S. Urbach, Phys. Rev. Lett. **81**, 4369 (1998).
- [4] I. Goldhirsch and G. Zanetti, Phys. Rev. Lett. **70**, 1619 (1993).
- [5] P.K. Haff, J. Fluid Mech. **134**, 401 (1983); J.T. Jenkins and S.B. Savage, *ibid.* **130**, 187 (1983); J.J. Brey, M.J. Ruiz-Montero, and D. Cubero, Phys. Rev. E **60**, 3150 (1999); T.P.C. van Noije and M.H. Ernst, Granular Matter **1**, 57 (1998); J.J. Brey, J.W. Dufty, C.S. Kim, and A. Santos, Phys. Rev. E **58**, 4638 (1998).
- [6] The temperature  $T$  here is not thermal, but actually a measure of the local energy density  $\mathcal{E}$  that is not accounted for by the local flow velocity:  $\rho T \equiv \mathcal{E} - \frac{1}{2} \rho u^2$ . Apart from this equation, it is not necessary to assume that this quantity  $T$  has any properties normally associated with temperature.
- [7] The question is similar to whether all of the physics of turbulence is captured by the Navier-Stokes equations, or whether one must, at some point, resort to a more microscopic theory.
- [8] P.K. Haff, J. Fluid Mech. **134**, 401 (1983).
- [9] B. Kim and G.F. Mazenko, J. Stat. Phys. **64**, 631 (1991). See also Ref. [10].
- [10] S.A. Hill and G.F. Mazenko, Phys. Rev. E **63**, 031303 (2001). The actual structure of the pressure  $P(\rho)$  in our previous paper is more complex than what we use here, but it does possess the high-density barrier to account for the ultimate incompressibility of the grains.
- [11] Others have dealt with the high-density limit by having the viscosity diverge as the density approaches its maximum value. See, for example, W. Losert *et al.*, Phys. Rev. Lett. **85**, 1428 (2000).
- [12] Some details about our methods: (1) Our Runge-Kutta method includes an adaptive time step; it, however, is rarely activated since we use a default time step that is suitably small. (2) We offset the velocities from other fields on the lattice such that the densities and temperatures may be considered to lie on the faces of the lattice while the horizontal (vertical) velocities lie on the vertical (horizontal) edges. (3) We have had great numerical difficulty with regions of very low density: such regions have a tendency to drift below zero density or generate large velocities in an unnatural fashion. We use an upwind technique to evaluate the equation  $\dot{\rho} = -\nabla(\rho u)$ , to prevent the density from becoming negative. In addition, we prevent mass from flowing out of any site with a density below some minimum value ( $\rho_{\min}=0.001$ ).
- [13] Our dimensionless density  $\rho$  should not be confused with the dimensionless packing fraction. For numerical convenience, our units of density have been scaled so that the random close-packed density corresponds to  $\rho_0=0.2$ . We will refer often to the ratio  $\rho/\rho_0$  to avoid confusion.
- [14] P. Deltour and J.-L. Barrat, J. Phys. I **7**, 137 (1997).
- [15] S. Luding and H.J. Herrmann, Chaos **9**, 673 (1999).
- [16] X. Nie, E. Ben-Naim, and S. Chen, Phys. Rev. Lett. **89**, 204301 (2002).
- [17] S. McNamara and W.R. Young, Phys. Rev. E **53**, 5089 (1996).